01 Nov 2011

C(naphthyl)-H Bond Activation by Rhodium: Isolation, Characterization and TD-DFT Study of the Cyclometallates

Achintesh Narayan Biswas

Purak K. Das

Sandip K. Sengupta

Amitava Choudhury
Missouri University of Science and Technology, choudhurya@mst.edu

et. al. For a complete list of authors, see https://scholarsmine.mst.edu/chem_facwork/2172

Recommended Citation

A. N. Biswas et al., "C(naphthyl)-H Bond Activation by Rhodium: Isolation, Characterization and TD-DFT Study of the Cyclometallates," *RSC Advances*, vol. 1, no. 7, pp. 1279-1286, The Royal Society of Chemistry, Nov 2011.
The definitive version is available at https://doi.org/10.1039/c1ra00572c

RSC Advances

Cite this: *RSC Advances*, 2011, **1**, 1279–1286

www.rsc.org/advances

PAPER

C(naphthyl)–H bond activation by rhodium: isolation, characterization and TD-DFT study of the cyclometallates†

Achintesh Narayan Biswas,[a] Purak Das,[a] Sandip Sengupta,[a] Amitava Choudhury[b] and Pinaki Bandyopadhyay*[a]

Received 9th August 2011, Accepted 9th August 2011
DOI: 10.1039/c1ra00572c

The C1(naphthyl)–H, C2(naphthyl)–H, C3(naphthyl)–H and C8(naphthyl)–H bonds of the naphthyl group present in a group of naphthylazo–2′–hydroxyarenes (H_2L) have been activated by $[Rh(PPh_3)_3Cl]$ in a toluene medium. Here the cyclometallation is accompanied by metal centered oxidation [Rh(I)→Rh(III)]. All the resulting cyclometallates $[Rh(PPh_3)_2(L)Cl]$ (**2**–**5**) have been isolated in a pure form. The characterization of the cyclometallates $[Rh(PPh_3)_2(L)Cl]$ have been done on the basis of spectral (IR, UV–vis, and FAB mass) data. The structures of the representative cyclometallates **2a**, **3a**, **4a**, **4b** and **5b** have been determined by X-ray diffraction. In all the cyclometallates, rhodium(III) is coordinated to naphthylazo–2′–hydroxyarenes *via* terdentate C(naphthyl), N(diazene), O(phenolato/naphtholato) donor centers & one chloride ion in a plane along with two axial *trans* PPh_3 molecules. Intermolecular association in the solid state is observed due to C–H···π and π···π interactions. Compounds show an oxidative response within 0.93 to 1.11 V (*vs.* SCE) and a reductive response at ~ −1.0 V (*vs.* SCE). Both the responses are based on the coordinated diazene function and are irreversible in nature, indicating limited stability of the oxidized and reduced species. The electronic structures of selected cyclometallates have been calculated using a TD-DFT model and the simulated spectra are consistent with the observed spectra of those cyclometallates.

Introduction

The activation of C–H bonds in organic compounds promoted by transition metal complexes has experienced a rapid growth in view of its diverse synthetic potential.[1] In this regard, the cyclometallation reaction, probably the mildest route for activating the C–H bond, has received increased attention.[2] Cyclometalation reactions have proven to be a powerful synthetic route, especially in the activation of C–H bonds, which are otherwise difficult to access.[3]

In general, the metal centres, precoordinated to a Lewis basic heteroatom group of the organic substrate, are brought in the vicinity of C–H bonds to be activated, which ultimately leads to the formation of a metal-carbon bond.[2a] The presence of more than one potential C–H activation site in a molecule often poses an interesting challenge regarding the selectivity of the process. The issue of regioselectivity can be addressed by attuning the hetroatom coordination to direct the metal ion to a site proximal to the selected C–H bond.[4]

The present work stems from our interest in C–H bond activation by transition metal complexes.[5] Herein, C(naphthyl)–H bond activation of a group of napthylazo–2′–hydroxyarenes (H_2L, 1) by rhodium has been reported. Wilkinson's catalyst $[Rh(PPh_3)_3Cl]$ has been specifically chosen as the metal precursor for its known ability to promote cyclometalation following an oxidative addition pathway,[6] thereby accommodating terdentate dianionic diazene substrates (H_2L, 1).[7] The preferential C(naphthyl)–H bond activation by rhodium has been explored by varying the position of the primary donor (diazene group) attached to the naphthyl group. Furthermore, an additional or auxiliary donor has been incorporated in the substrate molecule to examine its influence on the selectivity of the C(naphthyl)–H bond activation. The isolation, properties and molecular structure of the resulting cyclometallates have been described. The electronic structures of cyclometallates have been calculated using time dependent-density functional theory (TD-DFT).

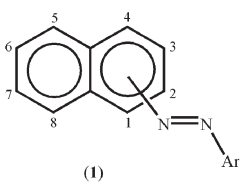

(1)

	Position of diazene (-N=N-)	Ar
H_2L^1	C_1	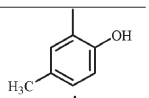
H_2L^2	C_1	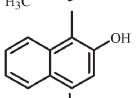
H_2L^3	C_2	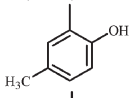
H_2L^4	C_2	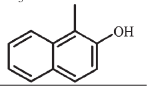

[a]*Department of Chemistry, University of North Bengal, Raja Rammohunpur, Siliguri, 734013, India. E-mail: pbchem@rediffmail.com; Fax: 91 353 2699001; Tel: 91 353 2776381*
[b]*Department of Chemistry, Missouri S & T, Rolla, MO, 65409, USA*

† Electronic supplementary information (ESI) available: Full description of the crystal packing of the cyclorhodates (ESI 1), cyclic-voltammetric data (ESI 2), Energies and percentage composition of the Mos (ESI 3). CCDC reference numbers, 772448, 772237, 772044, 772045 and 772238. For ESI and crystallographic data in CIF or other electronic format see DOI: 10.1039/c1ra00572c

Results and discussions

C(Naphthyl)–H bond activation by rhodium

Napthylazo–2′–hydroxyarenes (H_2L^1–H_2L^4) with diazene as the directing group offer quasi-equivalent metalation sites. When the primary donor (diazene) is attached to the C1of a naphthyl group, it offers two potentials sites for metallation, at C2 (*ortho*) and C8 (*peri*) leading to the formation of two isomeric cyclometallates. On the other hand, C3 and C1 are the probable sites of metalation when the directing diazene group is at C2 position.

Driven by the aim to examine the consequences of the substrate modifications on C(naphthyl)–H bond activation, reactions of the naphthylazoarenes (H_2L^1–H_2L^4) have been carried out with $[Rh(PPh_3)_3Cl]$ in refluxing toluene. The reaction proceeded smoothly and afforded the cyclorhodates (**2**–**5**) in decent yields. Elemental analysis and ^1H NMR spectral data are found to be consistent with the formation of rhodium(III) cyclometallates *via* metal based two-electron oxidation. In the case of 1–(2′–hydroxy–5′–methylphenylazo) naphthalene (H_2L^1), the reaction was found to be regiospecific in nature, affording a dark blue cyclometallate **2a** as the sole product (Scheme 1). Structure determination of **2a** by X-ray crystallography (Fig. 1) revealed that H_2L^1 is coordinated to rhodium(III) in a dianionic terdentate fashion *via* C2(naphthyl), N(diazene) and O(phenolato) donors. The C,N,O–coordinated ligand along with a chloride ion constitute an equatorial plane around the metal center, while the two PPh_3 occupy the remaining two axial *trans* positions. The Rh–C, Rh–N, Rh–O, Rh–P and Rh–Cl distances are in agreement with reported values.[7]

Thus, the complex $[Rh(PPh_3)_3Cl]$ regiospecifically activates the C2–H bond of the naphthyl group of H_2L^1 where the primary donor (–N=N–) is at C1 of the naphthyl ring and the auxiliary donor is the phenolic functional groups. To examine the effect of naphthol as an auxiliary donor on the activation of the C(naphthyl)–H bond by rhodium(I), 1–(2′–hydroxy-naphthylazo)naphthalene (H_2L^2) was chosen as substrate. Interestingly, the reaction of H_2L^2 with $[Rh(PPh_3)_3Cl]$ afforded a mixture of blue (**3a**) and pink (**3b**) compounds as products (Scheme 2). On the basis of elemental analysis and mass spectral data it is established that compounds (**3a** & **3b**) are isomeric. The molecular structure of the blue cyclometallate (**3a**) has been shown in Fig. 2. The compound **3a** shows a rhodium(III) center bonded to C2 of the naphthyl ring, N2 of the diazene functionality, O1 of the naphtholato fragment of the terdentate donor system and Cl1, along with two mutually *trans* triphenylphosphines in a distorted octahedral geometry.

Single crystals, suitable for X-ray crystallographic analysis of the *peri*-isomer **3b** could not be grown. The presence of the

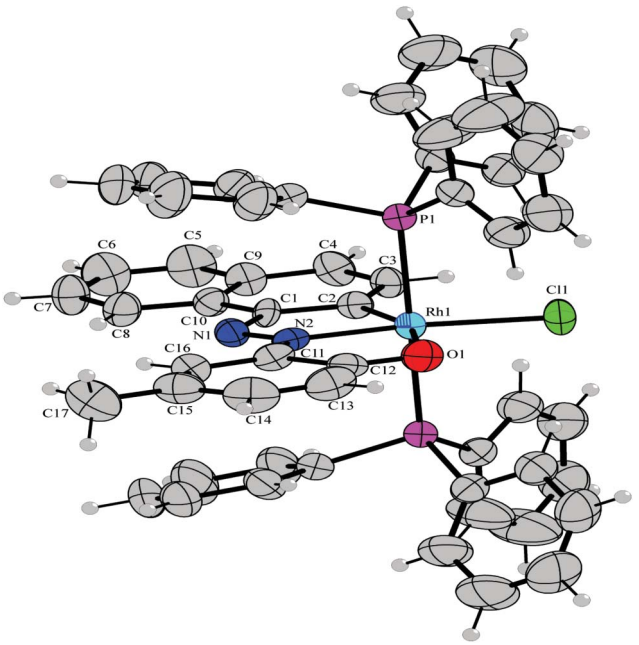

Fig. 1 ORTEP diagram of **2a**. Selected bond distances (Å): Rh1–C2, 1.904(6); Rh1–N2, 1.984(5); Rh1–O1, 2.288(5); Rh1–Cl1, 2.3673(10); Rh1–P1, 2.3835(6), N1–N2, 1.270(5). Selected angles (°): C2–Rh1–N2, 80.3(2); N2–Rh1–O1, 77.20(19); O1–Rh1–Cl1, 87.22(12); C2–Rh1–P1, 91.50(14); N2–Rh1–P1, 89.52(12); O1–Rh1–P1, 88.56(11); Cl1–Rh1–P1, 90.086(12).

naphthol group as an auxiliary donor, thus, ensures activation of both the C2(naphthyl)–H & C8(naphthyl)–H bonds by rhodium, whereas rhodium regiospecifically activates the C2(naphthyl)–H bond when the phenolic group is an auxiliary donor. The formation of isomeric cyclorhodates, **3a** & **3b**, can be rationalized considering the well known azo-hydrazo tautomerism displayed by naphthylazonaphthols in solution. The tautomeric behaviour of naphthylazonaphthol is well known[8] and it seems to play an important role in the selectivity of C–H bond activation. The azo-enol form of naphthylazonaphthol initially binds the metal center in the complex $[Rh(PPh_3)_3Cl]$ *via* oxidative insertion of rhodium into the O–H bond with concomitant dissociation of one triphenylphosphine, generating a reactive intermediate which activates the C2(naphthyl)–H bond only with simultaneous elimination of H_2 to afford the cyclometallate **3a**. On the other hand, the hydrazo-keto form of H_2L^2 binds the metal center in the complex $[Rh(PPh_3)_3Cl]$ *via* oxidative insertion of rhodium into N–H bond with simultaneous dissociation of one triphenylphosphine and produces a reactive intermediate,

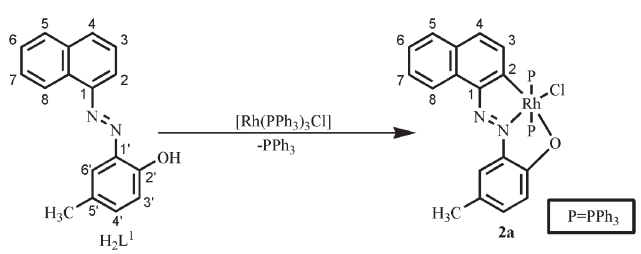

Scheme 1 Formation of the cyclorhodate **2a**.

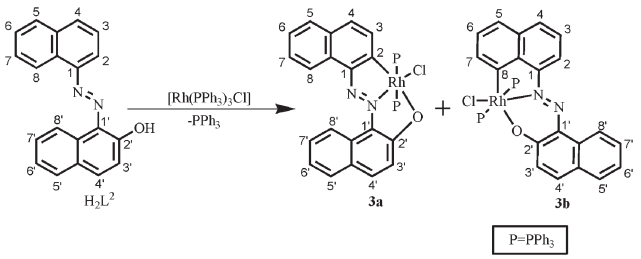

Scheme 2 Formation of the cyclorhodates **3a** and **3b**.

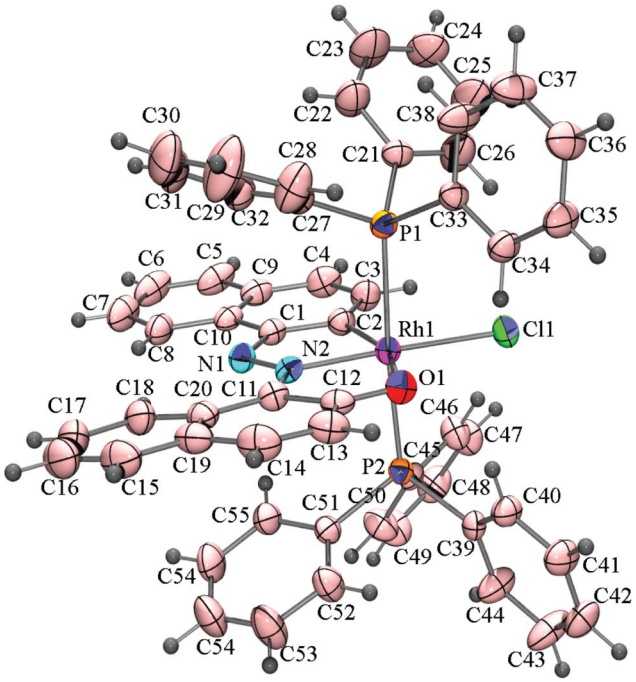

Fig. 2 ORTEP diagram of **3a** drawn at 50% probability. The solvent molecule has been omitted for clarity. Selected bond distances (Å): Rh1–C2, 2.002(5); Rh1–N2, 1.987(4); Rh1–O1, 2.189(3); Rh1–Cl1, 2.3895(13); Rh1–P1, 2.3719(14), Rh1–P2, 2.3874(13), N1–N2, 1.291(5). Selected angles (°): C2–Rh1–N2, 80.3(2); N2–Rh1–O1, 78.73 (14); N2–Rh1–P1, 92.93(11); C2–Rh1–P1, 89.91(14); O1–Rh1–P1, 88.83(9); N2–Rh1–P2, 91.78(11); C2–Rh1–P2, 90.33(14); O1–Rh1–P2, 92.65(9); C2–Rh1–P1, 89.91(14); P1–Rh1–P2, 175.25(5).

which activates the C8(naphthyl)–H bond and undergoes cyclometallation *via* elimination of H_2 resulting in the cyclometallate **3b** with a five-membered metallocarbocycle. The exclusive formation of the orthometallate **2a** occurs only in case of H_2L^1, which exists in azo-enolic form predominantly in solution.

The effect of the directing diazene group at the C2 position on the activation of C(naphthyl)–H bonds by rhodium(I) has also been examined. The reactions of $[Rh(PPh_3)_3Cl]$ with 2–(2′–hydroxy–5′–methylphenylazo)naphthalene (H_2L^3) and 2–(2′–hydroxy-napthylazo)naphthalene (H_2L^4) under identical conditions affords mixtures of cyclorhodates, **4a** & **4b**, and **5a** & **5b**, respectively. X-ray crystallographic analysis of the cyclorhodates **4a**, **4b** and **5b** have confirmed the regioselective activation of C1(naphthyl)–H and C3(naphthyl)–H bonds in the these complexes. The molecular structures of **4a**, **4b** and **5b** are shown in Fig. 3–5.

The probable steps behind the formation of the cyclometallates **4a** & **4b** are envisaged as follows. The azo-enol form of H_2L^3 binds $[Rh(PPh_3)_3Cl]$ *via* the oxidative insertion of rhodium into the O–H bond with the concomitant dissociation of one triphenylphosphine, generating a reactive intermediate, which has an equal chance to activate either the C1(naphthyl)–H or the C3(naphthyl)–H bond and undergoes cyclometallation *via* elimination of H_2 to afford a five membered metallocarbocycle, resulting in the formation of **4a** and **4b**. Similarly, the azo-enol form of H_2L^4 follows the same route, resulting in cyclometallates **5a** and **5b**. The hydrazo-keto form of H_2L^3 and H_2L^4 fails to provide any stable five-membered metallocarbocycles.

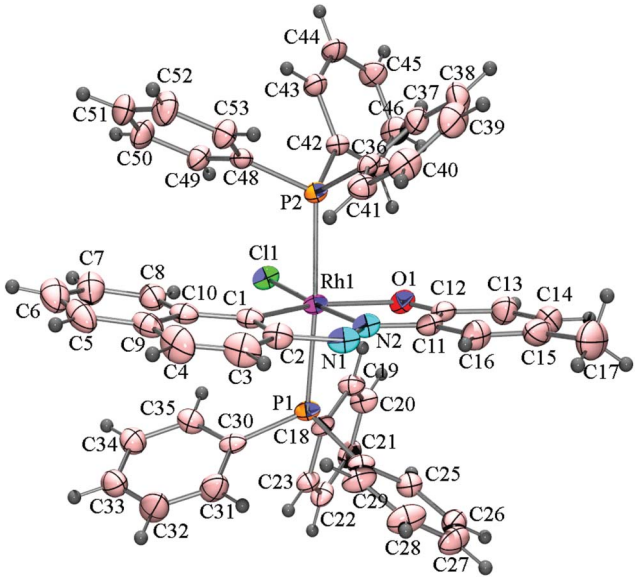

Fig. 3 ORTEP diagram of **4a** drawn at 50% probability. Selected bond distances (Å): Rh1–C1, 2.040(4); Rh1–N2, 1.938(3); Rh1–Cl1, 2.3755(12); Rh1–O1, 2.184(3); N1–N2, 1.283(3). Selected angles (°): C1–Rh1–N2, 78.82(16); N2–Rh1–O1, 80.19(13); P1–Rh1–Cl1, 87.93(4); O1–Rh1–Cl1, 93.91(8); O1–Rh1–P2, 93.41(7); C1–Rh1–P1, 90.44(10); N2–Rh1–P2, 93.16(9); P1–Rh1–P2, 174.11(4).

All the rhodium(III) cyclometallates uniformly display strong bands near 520, 690 and 750 cm^{-1} which are attributed to vibrations arising from the *trans*-$Rh(PPh_3)_2$ moiety. It is known that the *trans*-$M(PPh_3)_2$ fragments display such vibrations.[9] All the rhodium(III) cyclometallates exhibit various non-covalent

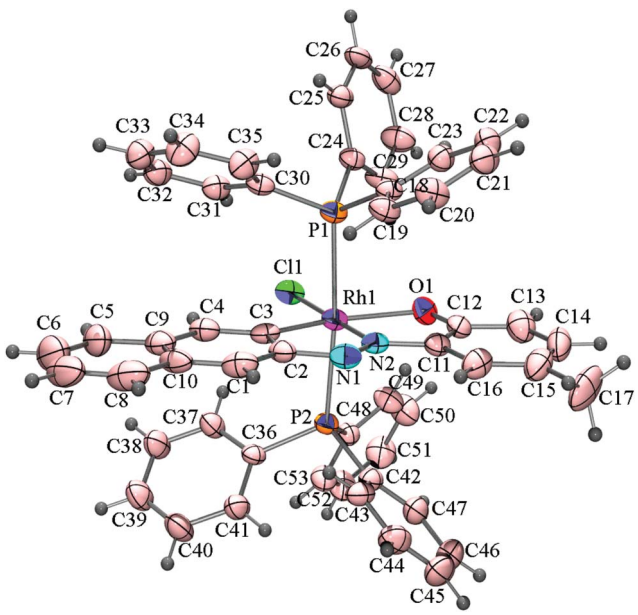

Fig. 4 ORTEP diagram of **4b** drawn at 50% probability. Selected bond distances (Å): Rh1–C3, 1.960(5); Rh1–N2, 1.961(4); Rh1–Cl1, 2.3824(11); Rh1–O1, 2.196(3); N1–N2, 1.280(4). Selected angles (°): C3–Rh1–N2, 79.9(2); N2–Rh1–O1, 80.51(17); P1–Rh1–Cl1, 88.74(4); O1–Rh1–Cl1, 98.80(9); O1–Rh1–P2, 94.16(8); C3–Rh1–Cl1, 100.76(16); C3–Rh1–P1, 88.94(12); N2–Rh1–P2, 92.24(10); P1–Rh1–P2, 174.81(5).

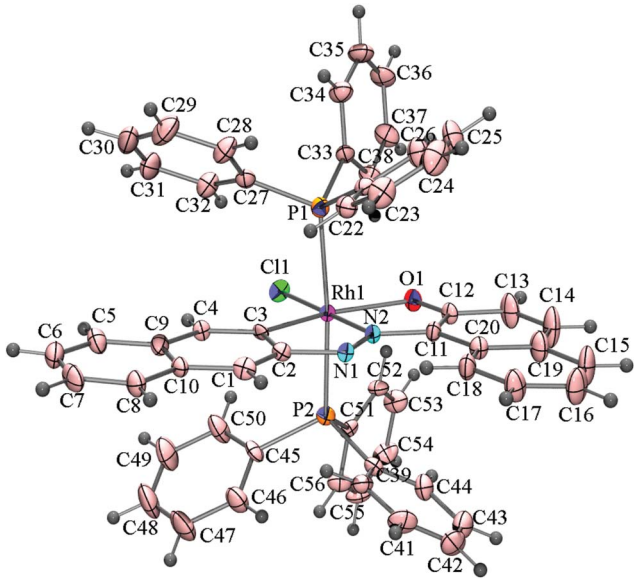

Fig. 5 ORTEP diagram of **5b** drawn at 50% probability. Selected bond distances (Å): Rh1–C3, 1.993(6); Rh1–N2, 1.968(5); Rh1–Cl1, 2.3731(18); Rh1–O1, 2.161 (5); N1–N2, 1.298(7). Selected angles (°): C3–Rh1–N2, 80.6(3); N2–Rh1–O1, 80.20(2); P1–Rh1–Cl1, 89.51(7); O1–Rh1–Cl1, 97.82(15); O1–Rh1–P2, 92.49(15); C3–Rh1–Cl1, 101.4(2); C3–Rh1–P1, 88.5(2); N2–Rh1–P2, 91.5(17); P1–Rh1–P2, 174.86(7).

interactions in the solid state. C–H···π, π···π and π stacking interactions between the aromatic rings have all been observed. Geometric parameters of all the interactions are compiled in the ESI.† Descriptions of the crystal packing have also been provided in the supporting information.

Electrochemistry

The electron transfer properties of the $[Rh(PPh_3)_2(L)Cl]$ complexes have been studied in an acetonitrile : dichloromethane (9 : 1) solution with the supporting electrolyte, NBu_4ClO_4 (0.1M), by cyclic voltammetry. All the complexes show an oxidative response to more positive potentials with respect to the SCE and a reductive response to negative ones. A representative voltammogram is shown in Fig. 6 and the voltammetric data is presented in Table S4, ESI.† Both responses are believed to be centered on the coordinated azo ligand.[7] The oxidative response, observed within 0.93 to 1.11 V *vs.* SCE, is irreversible in nature, as evidenced by the fact that the cathodic peak current (i_{pc}) is less than the anodic peak current (i_{pa}). The one-electron nature of this oxidation has been verified by comparing its current height (i_{pa}) with that of the standard ferrocene–ferrocenium couple under identical experimental conditions. The reductive response, displayed at around −0.9 V *vs.* SCE, is also irreversible in nature. The cyclic voltammetric studies thus show that these rhodium(III) organometallics are quite stable, while the oxidized and reduced species undergo rapid decomposition.

TD-DFT study

The rhodium(III) cyclometallates (**2a**–**5b**) are soluble in common organic solvents. The electronic spectra of the cyclometallates, recorded in dichloromethane show several intense absorptions in the visible and ultraviolet regions. Electronic spectra of the

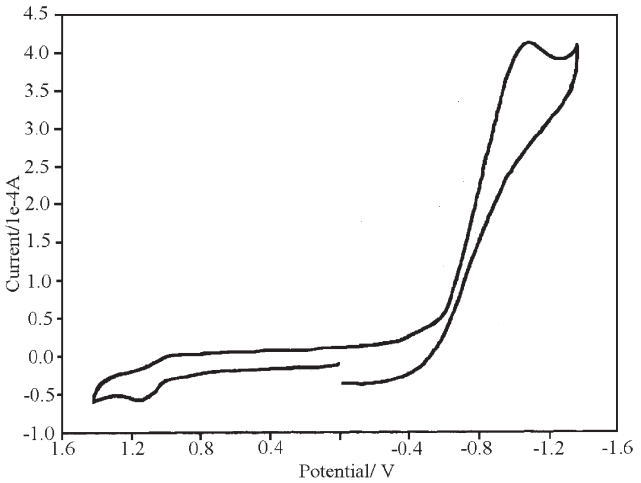

Fig. 6 Cyclic voltammogram of $[Rh(PPh_3)_2(L^1)Cl]$, **4a** in an acetonitrile : dichloromethane (9 : 1, v/v) solution (0.1M NBu_4ClO_4) at scan rate 50 mV s^{-1}.

rhodium(III) cyclometallates are shown in Fig. 7. Spectral data are presented in the Experimental Section. The absorption bands observed in the visible and ultraviolet region with a high molar extinction coefficient have been reported as metal–to–ligand charge-transfer transitions (MLCT) and intraligand charge-transfer transitions respectively.[7] The absorptions in the ultraviolet region were attributed to the usual n→π* and π→π* transitions occurring within the ligand orbitals.

The time-dependent DFT (TD-DFT) calculations of the representative rhodium(III) cyclometallates (**4a** & **4b**) has been done to gain further insight into the nature of the absorptions. Only the singlet excited states have been calculated. Excitation energies and oscillator strengths for the various absorption bands have been reported together with the composition of the solution vectors in terms of most relevant transitions (Table 1).

It is revealed that the HOMO is delocalized over the naphthylazophenolato fragment (Fig. 8 and Tables S5 and S6, ESI,†) for both **4a** & **4b**. The HOMO−1 has significant contributions from the rhodium d orbitals in **4a** & **4b** (41.75 and 44.69% respectively). The lowest unoccupied molecular orbitals

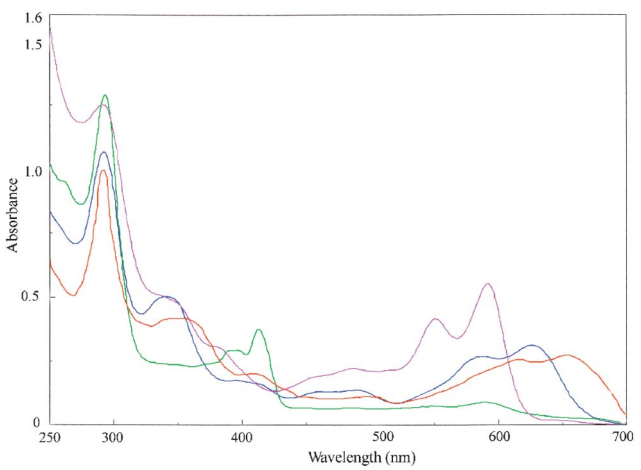

Fig. 7 Electronic spectra of the cyclorhodates **4a** (orange), **4b** (blue), **5a** (green) and **5b** (pink) in dichloromethane.

Table 1 Selected TD-DFT calculations of excitation energies, wavelengths (λ), oscillator strengths (f) and compositions of the low-lying singlet states in dichloromethane solution for the cyclometallates **4a** and **4b**

Code	State	Energy (eV)	λ_{cal} (nm)	λ_{exp} (nm)	Oscillator strength (f)	Composition	Character
4a	S_1	1.8090	686	627	0.075	HOMO→LUMO (93.5%)	ILCT+LLCT
	S_{14}	3.0267	410	–	0.072	HOMO−5→LUMO (55.5%) HOMO→LUMO+7 (12.4%) HOMO−4→LUMO (12.2%)	LLCT+MLCT
	S_{44}	3.5650	348	340	0.194	HOMO−5→LUMO+1 (33.8%) HOMO−4→LUMO+1 (33.5%)	LLCT+LMCT
	S_{59}	3.8183	325	292	0.068	HOMO−6→LUMO+1 (51.9%) HOMO−3→LUMO+4 (27.5%)	LLCT+MLCT
4b	S_1	1.8920	656	668	0.027	HOMO→LUMO (61.7%) HOMO−2→LUMO (27.1%)	ILCT+LLCT
	S_3	2.2337	556	–	0.088	HOMO−2→LUMO (61.1%) HOMO→LUMO (22.5%)	LLCT+ILCT
	S_5	2.5167	493	–	0.041	HOMO−3→LUMO (78.7%) HOMO−4→LUMO (10.4%)	LLCT+MLCT
	S_{12}	3.0187	411	–	0.072	HOMO−5→LUMO (44.2%) HOMO→LUMO+5 (21.1%) HOMO−4→LUMO (10.6%)	LLCT+ILCT+MLCT
	S_{49}	3.6229	343	340	0.125	HOMO→LUMO+14 (24.8%) HOMO−5→LUMO+1 (23.0%) HOMO−17→LUMO (20.7%)	LLCT

(LUMO) are almost entirely localized over the ligand moiety. The isomers have been found to differ in the energy of the HOMO, with a lower energy in the case of **4b** than that for **4a**. The HOMO–LUMO gaps have been computed to be 1.44 and 1.56 eV respectively. The calculated lowest energy transition wavelengths of **4a** & **4b** are 686 nm and 656 nm respectively. The results for these absorptions agree with those determined experimentally by UV–vis spectroscopy (Table 1). In **4a**, the lowest energy transition is HOMO→LUMO (93.5%), which corresponds to an intraligand charge transfer transition (LLCT). In **4b**, the main transitions in the lowest energy region are HOMO→LUMO (61.7%) and HOMO−2→LUMO (27.1%). The HOMO–LUMO gap is computed to be 1.44 eV. The most intense transition is observed in **4a** in the UV region (*ca.* 325 nm) and involves excitation from HOMO and HOMO−3 to LUMO+1 and LUMO+3 respectively, with predominantly intraligand π–π* character and a small admixture of MLCT. Similarly, in the case of **4b**, the same absorption band appears at 340 nm and involves excitation from HOMO, HOMO−5 and HOMO−17 to LUMO+14, LUMO+1 and LUMO respectively, with predominantly intraligand π–π* character and a small admixture of MLCT.

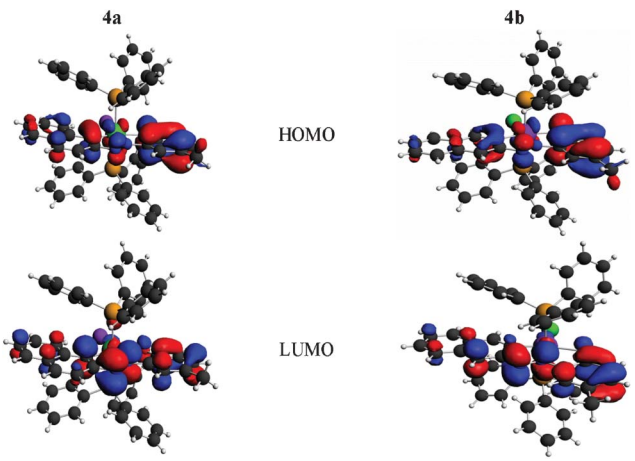

Fig. 8 Partial molecular orbital diagram of the cyclorhodates **4a** and **4b**.

Conclusions

The activation of different C(naphthyl)–H bonds *viz.* C1–H, C2–H, C3–H and C8–H bonds in naphthylazo–2′–hydroxyarenes (H_2L, **1**) have been achieved by rhodium(I) following an oxidative addition pathway affording rhodium(III) complexes. The different positions of the directing primary donor (the diazene functional group) and the incorporation of suitable auxiliary donors govern the selectivity of the C–H bond activation. The azo-hydrazo tautomerism of naphthylazo–2′–hydroxyarenes also plays an important role in the observed selectivity. Regiospecific C2(naphthyl)–H activation has been achieved by rhodium(I) when the primary donor (diazene) is at C1 and the auxiliary donor is phenol, whereas the presence of naphthol as the auxiliary donor leads to the regioselective activation of C2(naphthyl)–H & C8(naphthyl)–H bonds. Regioselective activation of C1(naphthyl)–H & C3(naphthyl)–H bonds have been achieved by rhodium(I), where the primary donor (diazene) is at C2 and the auxiliary donor is phenol or naphthol. The origin of the electronic transitions in the cyclorhodates has been investigated by TD-DFT. The calculations corroborate the experimental results. Based on the TD-DFT calculations, the lowest energy transitions in cyclorhodates have been shown to be intra-ligand charge transfer transitions occurring in the terdentate dianionic naphthylazo–2′–hydroxyarenes ligands.

Experimental Section

Materials

$RhCl_3.nH_2O$ was obtained from Arora-Matthey, Kolkata. Complex $[Rh(PPh_3)_3Cl]$ was prepared following a reported method.[10] Solvents and chemicals used for the syntheses were of analytical grade. Tetrabutylammonium perchlorate

for the electrochemical work was synthesized following a reported method.[11]

Physical measurements

Elemental microanalyses (C, H and N) were performed by either a Perkin-Elmer (Model 240C) or a Heraeus Carlo Erba 1108 elemental analyzer. The IR and Electronic spectra were recorded on a Jasco 5300 FT-IR spectrophotometer and a JASCO V-500 spectrophotometer respectively. NMR spectra were obtained by a Bruker DPX 300 NMR Spectrometer. Electrochemical measurements were performed by a computer controlled PAR model (VERSASTAT II) electrochemical instrument. A platinum disc working electrode, a platinum wire auxiliary electrode and an aqueous saturated calomel reference electrode (SCE) were used in the cyclic voltammetry experiments. All electrochemical experiments were performed under a dinitrogen atmosphere at 298 K in 1 : 9 dichloromethane/acetonitrile using [nBu$_4$N][ClO$_4$] (TBAP) as the supporting electrolyte. The reported potentials are uncorrected for the junction potential.

Synthesis of the ligands

Compounds (H_2L^1–H_2L^4) were synthesized by published procedures.[12,5c]

Isolation of rhodium(III) cyclometallates

Isolation of [Rh(L^1)(PPh$_3$)$_2$Cl] (2a). The compound 1–(2′–hydroxy–5′–methylphenylazo)naphthalene (H_2L^1) (0.026 g, 0.1 mmol) was dissolved in 50 cm^3 toluene and the solution was purged with dinitrogen for 15 min. Then [Rh(PPh$_3$)$_3$Cl] (0.1 g, 0.1 mmol) was added slowly to solution and the whole mixture was refluxed under a dinitrogen atmosphere for six hours. The solvent was evaporated under reduced pressure and the crude green solid was dissolved in dichloromethane and was subjected to purification by thin layer chromatography on a silica plate. With a mixture of petroleum benzene/ethyl acetate (20 : 1,v/v) as eluant a bluish green band was isolated and extracted with acetonitrile. Evaporation of the solvent afforded the titled compound. Yield: 55%. Anal. Calc. for $C_{53}H_{42}N_2OClP_2Rh$: C, 68.95; H, 4.59; N, 3.03. Found: C, 68.80; H, 4.82; N, 2.92%. ^{1}H NMR ($CDCl_3$):δ: 1.76 (s,3H, aryl CH_3); aromatic protons: 5.89 (s, 1H), 6.19 (d, 1H, J = 6.6 Hz), 6.45 (dd, 1H, J = 6.6 Hz), 6.87 (d, 1H, J = 6.6 Hz), 7.06 (m, 11H), 7.18 (m, 9H), 7.24 (m, 1H), 7.32 (t, 1H), 7.45 (m, 12H), 8.27 (d, 1H, J = 6 Hz). IR (KBr): ν 1402 cm^{-1} (–N=N–). UV–vis (dichloromethane), λ_{max}/nm (ε/M^{-1} cm^{-1}): 676 (11,950), 627 (9,600), 290(40,300). MS: m/z: 923 [M]$^+$, 398 [M–2PPh$_3$]$^+$.

Isolation of [Rh(L^2)(PPh$_3$)$_2$Cl] (3a & 3b). Isolation of the isomeric cyclometallates **3a** and **3b** were achieved following the same procedure as above, using H_2L^2 instead of H_2L^1. Here a mixture of petroleum benzene and ethyl acetate (10 : 1 v/v) has been used as eluent . A blue fraction and a pink–violet fraction were obtained. The bands were separated and extracted with acetonitrile.

3a. Yield 28%. Anal. Calc. for $C_{56}H_{42}N_2OClP_2Rh$: C, 70.12; H, 4.41; N, 2.92. Found: C, 69.79; H, 4.60; N, 2.86%.^{1}H NMR ($CDCl_3$):δ: 6.48 (d,1H), 6.99 (m,7H), 7.26 (m, 12H), 7.45 (m, 9H), 7.67 (m, 10H), 7.95 (d, 1H), 8.10 (d, 1H, J = 6 Hz), 8.21 (d, 1H, J = 6 Hz). IR (KBr): ν 1405 cm^{-1} (–N=N–). UV–vis (dichloromethane), λ_{max}/nm (ε/M^{-1} cm^{-1}): 289 (63,400), 378 (17,200), 404 (13,600), 604 (19,100), 655 (25,600). MS: m/z 958 [M]$^+$.

3b. Yield 45%. $C_{56}H_{42}N_2OClP_2Rh$: C, 70.12; H, 4.41; N, 2.92. Found: C, 70.09; H, 4.56; N, 3.02%. ^{1}H NMR ($CDCl_3$):δ: 6.42 (d, 1H, J = 6.3 Hz), 7.02 (m, 12H), 7.21 (m, 12H), 7.37 (m, 13H), 7.55 (m, 2H), 7.81 (d, 1H, J = 6 Hz), 8.12 (d, 1H, J = 7.8 Hz). IR (KBr): ν 1395 cm^{-1} (–N=N–). UV–vis (dichloromethane), λ_{max}/nm (ε/M^{-1} cm^{-1}): 278 (80,300), 560 (28,200), 602 (32,400). MS: m/z 958 [M]$^+$, 661[M−(PPh$_3$+Cl)]$^+$.

Isolation of [Rh(L^3)(PPh$_3$)$_2$Cl] (4a & 4b). Isolation of the isomeric cyclometallates **4a** and **4b** were achieved following the same procedure as above, using H_2L^3 instead of H_2L^1. In this case purification of the reaction mixture by thin layer chromatography (silica, petroleum benzene/ethyl acetate, 10 : 1 v/v) afforded a sky blue (**4a**) fraction and a greenish blue (**4b**) fraction. The bands were separated and extracted with acetonitrile.

4a. Yield 20%. Anal. Calc. for $C_{53}H_{42}N_2OClP_2Rh$: C, 68.95; H, 4.59; N, 3.03. Found: C, 68.76; H, 4.62; N, 3.02%.^{1}H NMR ($CDCl_3$):δ: 1.78 (s,3H, aryl CH_3), 5.93 (s,1H), 6.25 (d, 1H, J = 6.3 Hz), 6.56 (dd, 1H), 6.94 (t, 5H) 7.05–7.15 (m, 5H), 7.14–7.21 (m, 15H), 7.39–7.43 (m, 10H), 8.4 (d, 1H, J = 8.1 Hz). IR (KBr): ν 1402 cm^{-1} (–N=N–). UV–vis (dichloromethane), λ_{max}/nm (ε/M^{-1} cm^{-1}): 292 (47,500), 340 (22,300), 584 (12,000), 627 (9,600). MS: m/z 922 [M]$^+$.

4b. Yield 35%. Anal. Calc. for $C_{53}H_{42}N_2OClP_2Rh$: C, 68.95; H, 4.59; N, 3.03. Found: C, 69.10; H, 4.69; N, 2.88%.^{1}H NMR ($CDCl_3$): δ: 1.78 (s,3H, aryl CH_3), 5.52 (d, 1H), 6.04 (m, 3H), 6.93–7.03 (m, 15H), 7.28–7.67 (m, 20H). IR (KBr): ν (–N=N–) 1408 cm^{-1}. UV–vis (dichloromethane), λ_{max}/nm (ε/M^{-1} cm^{-1}): 292 (15,500), 340 (9,500), 624 (3,600), 668 (5,100). MS: m/z 922 [M]$^+$, 660 [M–PPh$_3$]$^+$, 626 [M–(PPh$_3$+Cl)]$^+$.

Isolation of [Rh(L^4)(PPh$_3$)$_2$Cl] (5a & 5b). Isolation of the isomeric cyclometallates **5a** and **5b** were achieved following the same procedure as above, using H_2L^4 instead of H_2L^1. In this case purification of the reaction mixture by thin layer chromatography (silica, petroleum benzene/ethyl acetate, 20 : 1 v/v) afforded a blue (**5a**) fraction and a purple (**5b**) fraction. The bands were separated and extracted with acetonitrile.

5a. Yield: 20%. Anal. Calc. for $C_{56}H_{42}N_2OClP_2Rh$: C, 70.12; H, 4.41; N, 2.92. Found: C, 70.31; H, 4.45; N, 3.10%.^{1}H NMR ($CDCl_3$):δ: 6.56 (d, 1H, J = 6.0 Hz), 7.12–7.18 (m, 11H), 7.20–7.39 (m, 15H), 7.40 (m, 5H), 7.45–7.54 (m, 8H), 7.64 (s, 1H), 8.54 (d, 1H, J = 6.6 Hz). IR (KBr): ν 1405 cm^{-1} (–N=N–). UV-vis (dichloromethane), λ_{max}/nm (ε/M^{-1} cm^{-1}): 261 (59,600), 293 (80,500), 391 (18,500), 413 (23,600), 589 (5,800). MS: m/z 958 [M]$^+$.

5b. Yield: 72%. Anal. Calc. for $C_{56}H_{42}N_2OClP_2Rh$: C, 70.12; H, 4.41; N, 3.70. Found: C, 70.31; H, 4.45; N, 3.61%. ^{1}H NMR ($CDCl_3$):δ: 6.42 (d, 1H, J = 6.6 Hz), 7.10 (s, 1H), 7.20–7.31 (m, 15H), 7.34–7.51 (m, 18H), 7.71 (m, 6H, J = 8.1 Hz), 8.62 (d, 1H, J = 6.3 Hz). IR (KBr): ν 1395 cm^{-1} (–N=N–). UV–vis (dichloromethane), λ_{max}/nm (ε/M^{-1} cm^{-1}): 292 (25,200), 348^{sh} (9,400), 384 (5,400), 550 (8,400), 592 (11,600). MS: m/z 958 [M]$^+$.

Table 2 Crystal data and structure refinement for the cyclorhodates **2a**, **3a**, **4a**, **4b** and **5b**.

Compound reference	**3a2a**	**3a**. CH_2Cl_2	**4a**	**4b**	**5b**
Chemical formula	$C_{53}H_{42}ClN_2OP_2Rh$	$C_{57}H_{44}Cl_3N_2OP_2Rh$	$C_{53}H_{42}ClN_2OP_2Rh$	$C_{53}H_{42}ClN_2OP_2Rh$	$C_{56}H_{42}ClN_2OP_2Rh$
Formula Mass	923.19	1044.14	923.19	923.19	959.27
Crystal system	Monoclinic	Monoclinic	Triclinic	Triclinic	Monoclinic
a/Å	24.4771(3)	17.5179(2)	11.116(3)	11.8442(2)	11.905(3)
b/Å	9.2446(2)	16.35860(10)	11.742(4)	11.9633(3)	17.478(4)
c/Å	21.62350(10)	18.225	18.141(6)	17.3738(4)	22.043(5)
α (°)	90.00	90.00	108.857(4)	72.1650(10)	90.00
β (°)	116.3650(10)	109.9790(10)	99.704(5)	70.5110(10)	95.527(4)
γ (°)	90.00	90.00	100.613(5)	79.4750(10)	90.00
Unit cell volume/Å^3	4384.03(11)	4908.42(6)	2135.2(11)	2200.31(8)	4565.2(17)
T/K	293(2)	298(2)	293(2)	293(2)	293(2)
Space group	*C*2/*c*	*P*2(1/*c*	*P*$\bar{1}$	*P*$\bar{1}$	*P*21/*n*
No. of formula units per unit cell, *Z*	4	4	2	2	4
No. of reflections measured	8710	20154	20530	15152	42204
No. of independent reflections	3148	7005	7501	3911	7893
R_{int}	0.0299	0.0596	0.0430	0.0444	0.0666
Final R_1 values ($I > 2\sigma(I)$)	0.0277	0.0459	0.0516	0.0301	0.0967
Final $wR(F^2)$ values ($I > 2\sigma(I)$)	0.0644	0.1062	0.1077	0.0548	0.1962
Final R_1 values (all data)	0.0372	0.0844	0.0712	0.0489	0.0999
Final $wR(F^2)$ values (all data)	0.0684	0.1264	0.1151	0.0619	0.1981
Goodness of fit on F^2	1.048	0.991	1.048	1.009	1.172

Crystallography

Single crystals of complexes **2a** and **3a** were obtained by the slow diffusion of a dichloromethane solution of the complexes into n-hexane, whereas the single crystals of the cyclometallates **4a**,**4b** and **5b** were obtained by slow evaporation from the acetonitrile extract of the compounds. Crystallographic and refinement data for the reported structures† are presented in Table 2. Data on the crystals was collected on a Bruker SMART 1000 CCD area-detector diffractometer using graphite monochromated Mo-Kα (λ = 0.71073 Å) radiation by ω scan. The structure was solved by direct methods using SHELXS-97[13] and difference Fourier syntheses and refined with SHELXL97 package incorporated in WinGX 1.64 crystallographic collective package.[14] All the hydrogen positions for the compound were initially located in the difference Fourier map, and for the final refinement, the hydrogen atoms were placed geometrically and held in the riding mode. The last cycles of refinement included atomic positions for all the atoms, anisotropic thermal parameters for all non-hydrogen atoms and isotropic thermal parameters for all the hydrogen atoms. Full-matrix-least-squares structure refinement against $|F^2|$ molecular geometry calculations were performed with PLATON,[15] and molecular graphics were prepared using ORTEP-3.[16]

Method and Computational Details

The calculations have been performed within the TDDFT formalism as implemented in ADF2007.[17] Two approximations are generally made: one for the XC potential, and one for the XC kernel, which is the functional derivative of the time-dependent XC potential with respect to density. We used LDA (local density approximation) including the VWN parametrization[18] in the SCF step and Becke[19] and Perdew–Wang[20] gradient corrections to the exchange and correlation respectively and Adiabatic local Density Approximation (ALDA) for the XC kernel, in the post-SCF step. TD-DFT calculations have been performed with the uncontracted triple-STO basis set with a polarization function for all atoms. In the calculation of the optical spectra, 70 lowest spin-allowed singlet–singlet transitions have been taken into account. Transition energies and oscillator strengths have been interpolated by a Gaussian convolution with a σ of 0.2 eV. Solvent effects were modelled by the "Conductor-like Screening Model" (COSMO)[21] of solvation as implemented in ADF.

Acknowledgements

The financial supports from CSIR and Department of Science & Technology (DST), New Delhi are gratefully acknowledged.

References

1 (*a*) R.H. Crabtree, *J. Chem. Soc., Dalton Trans.*, **2001**, 2437; (*b*) J.A. Labinger and J.E. Bercaw, *Nature*, 2002, **417**, 507; (*c*) I. Omae, *Coord. Chem. Rev.*, 2004, **248**, 995; (*d*) A.E. Shilov, G.B. Shul'pin, *Activation and Catalytic Reactions of Saturated Hydrocarbons in the Presence of Metal Complexes*, Kluwer Academic Publishers, Dordretch, Germany, 2000; (*e*) W.D. Jones, *Acc. Chem. Res.*, 2003, **36**, 140; (*f*) D. Fiedler, D.H. Leung, R.G. Bergman and K.N. Raymond, *Acc. Chem. Res.*, 2005, **38**, 351; (*g*) M. Lersch and M. Tilset, *Chem. Rev.*, 2005, **105**, 2471; (*h*) E. Carmona, M. Paneque, L.L. Santos and V. Salazar, *Coord. Chem. Rev.*, 2005, **249**, 1729; (*i*) R.H. Crabtree, *J. Organomet. Chem.*, 2004, **689**, 4083; (*j*) R. Giri, B.-F. Shi, K.M. Engle, N. Maugel and J.-Q. Yu, *Chem. Soc. Rev.*, 2009, **38**, 3242.

2 (*a*) M. Albrecht, *Chem. Rev.*, 2010, **110**, 576; (*b*) G. Dyker, *Angew. Chem., Int. Ed.*, 1999, **38**, 1699; (*c*) Y. Guari, S. Sabo-Etienne and B. Chaudret, *Eur. J. Inorg. Chem.*, **1999**, 1047; (*d*) V. Ritleng, C. Sirlin and M. Pfeffer, *Chem. Rev.*, 2002, **102**, 1731; (*e*) A.D. Ryabov, *Chem. Rev.*, 1990, **90**, 403; (*f*) B.A. Arndtsen, R.G. Bergman, T.A. Mobley and T.H. Peterson, *Acc. Chem. Res.*, 1995, **28**, 154.

3 (*a*) J. Dupont, C.S. Consorti and J. Spencer, *Chem. Rev.*, 2005, **105**, 2527; (*b*) M.E. van der Boom and D. Milstein, *Chem. Rev.*, 2003, **103**, 1759; (*c*) M. Albrecht and G. van Koten, *Angew. Chem., Int. Ed.*, 2001, **40**, 3750.

4 (*a*) W. Clegg, S.H. Dale, E. Hevia, G.W. Honeyman and R.E. Mulvey, *Angew. Chem., Int. Ed.*, 2006, **45**, 2370; (*b*) W. Clegg, S.H. Dale, R.W. Harrington, E. Hevia, G.W. Honeyman and R.E. Mulvey, *Angew. Chem., Int. Ed.*, 2006, **45**, 2370.

5 (*a*) D.N. Neogi, P. Das, A.N. Biswas and P. Bandyopadhyay, *Polyhedron*, 2006, **25**, 2149; (*b*) D.N. Neogi, A.N. Biswas, P. Das, R. Bhawmick and P. Bandyopadhyay, *Inorg. Chim. Acta*, 2007, **360**, 2181; (*c*) A.N. Biswas, P. Das, V. Bagchi, A. Choudhury and P. Bandyopadhyay, *Eur. J. Inorg. Chem.*, 2011, DOI: 10.1002/ejic.

6 B. Rybtchinsky, R. Cohen, Y. Ben-David, J.M.L. Martin and D. Milstein, *J. Am. Chem. Soc.*, 2003, **125**, 11041.
7 *Cyclometallation of structurally related 2-(arylazo)phenols with [Rh(PPh3)3Cl] has been reported earlier.* See S. Dutta, S.M. Peng, S. Bhattacharya, *J. Chem. Soc., Dalton Trans.*, 2000, 4623.
8 R.A. Cox and E. Buncel, *The chemistry of hydrazo, azo and azoxy groups*, ed. S. Patai, Wiley, London, 1975, ch. 18.
9 (*a*) S. Bhattacharya and C.G. Pierpont, *Inorg. Chem.*, 1991, **30**, 1511; (*b*) S. Bhattacharya and C.G. Pierpont, *Inorg. Chem.*, 1991, **30**, 2906; (*c*) A. Das, F. Basuli, S.-M. Peng and S. Bhattacharya, *Polyhedron*, 1999, **18**, 2729.
10 J.A. Osborn and G. Wilkinson, *Inorg. Synth.*, 1967, **10**, 67.
11 D.T. Sawyer, J.L. Roberts, Jr., *Experimental Electrochemistry for Chemists*, Wiley, New York, 1974; pp. 167-215.
12 B.S. Furniss, A.J. Hannaford, V. Rogers, P.W.G. Smith, A.R. Tatchell (ed.) *Vogel's Text Book of Practical Organic Chemistry, fouth ed.*, ELBS and Longman Group Ltd., London, 1978.
13 G.M. Sheldrick, *Acta. Cryst.*, 2008, **A64**, 112.
14 L.J. Farrugia, *WinGX Version 1.64, An Integrated System of Windows Programs for the Solution, Refinement and Analysis of Single-Crystal X-ray Diffraction Data*, Department of Chemistry, University of Glasgow, 2003.
15 PLATON: A.L. Spek, *J. Appl. Crystallogr.*, 2003, **36**, 7.
16 L.J. Farrugia, *J. Appl. Crystallogr.*, 1997, **30**, 565.
17 The ADF program system was obtained from Scientific Computing and Modeling, Amsterdam (http://www.scm.com/). For a description of the methods used in ADF, see: G. T. Velde, F. M. Bickelhaupt, E. J. Baerends, C. F. Guerra, S. J. A. Van Gisbergen, J. G. Snijders and T. Ziegler, *J. Comput. Chem.*, 2001, **22**, p. 931.
18 S.H. Vosco, L. Wilk and M. Nusair, *Can. J. Phys.*, 1980, **58**, 1200.
19 A.D. Becke, *Phys. Rev.*, 1988, **A38**, 3098.
20 J.P. Perdew and Y. Wang, *Phys. Rev.*, 1992, **B45**, 13244.
21 (*a*) A. Klamt and G.J. Schüürmann, *J. Chem. Soc., Perkin Trans. 2*, **1993**, 799; (*b*) A. Klamt and V. Jonas, *J. Chem. Phys.*, 1996, **105**, 9972.